Descartes, Plateau, and sea urchins

M. Abou Chakra & J. R. Stone
Department of Biology: Computational Biology,
McMaster University, Canada

Abstract

Sea urchin skeletons (tests) exhibit pentamerous symmetry, a pattern that emerges from the beautiful and intricate arrangements among the plates of which they are composed. Plate patterns and test shapes have proven difficult to explain and describe solely on the basis of any one process. Using theoretical morphology, the discipline that involves using mathematical modelling and computer simulation to describe growth and form, we introduce a new computational model that utilises the manner with which soap bubbles interact in close-packing formation to emulate plate addition, shift, gapping and growth. The computational model is governed by close-packing configuration (Descartes circle theorem) and soap bubble interactions (Plateau's Laws). Through this analogy, our computational model can be used to describe the evolutionary morphological changes observed in sea urchin skeletons.
Keywords: skeleton, soap bubbles, growth, computational model, echinoid test.

1   Introduction

D'Arcy Thompson's *On Growth and Form* illustrates how physical principles can be employed to explain patterns observed in nature, including basaltic columns, turtle shells, insect wings, sea urchin skeletons and the infamous honeycomb cells, fig. 1 [1].

Thompson conceptualised the use of soap bubbles to model several biological patterns that occur in nature. Thompson considered physical forces operating in living systems, a subject he found lacking in biological research [1]. He showed that the hexagonal patterns in basaltic columns and honeycombs can be explained by considering the surface tension associated with the dynamics of a fluid [1]. Basaltic columns develop via a molten lava state; the hive wax film is added as a viscous fluid [1].

Sea urchin skeleton exhibit patterns and shapes which attracted the attention of many researchers and, over the last century, only 7 models have been proposed to explain or describe skeleton growth: [1–7]. Sea urchin skeletons display patterns similar to the basaltic columns and honeycomb cells, fig. 1 [1]. Thompson conceptualised using soap bubbles as an analogy to explain such biological patterns [1]. In the current study, we present the first complete analysis using soap bubble interactions and close-packing arrangements and create a computational model that can be used to explain observed patterns in sea urchin skeletons over time.

a   b   c
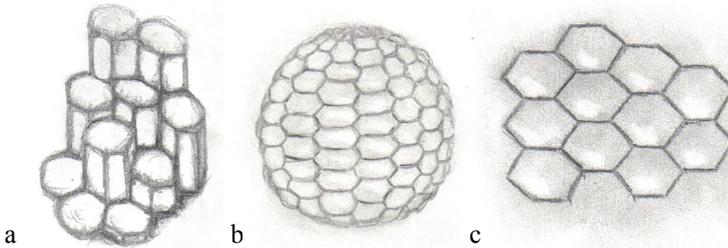
Figure 1:   Illustrations of natural phenomena a) basaltic columns (adapted from [1]), b) archaic sea urchin skeleton *Bothriocidaris* (adapted from [8]), and c) honeycomb cells.

2   Plateau and soap bubbles

For centuries, soap bubbles have captivated some biologists (Thompson with coalescence patterns), physicists (Plateau, Boys, and Isenberg with soap films), and mathematicians (Euler with area minima). Theoretical work was introduced by Plateau, who used wire frames to explain soap bubble interfaces [9, 10]. Plateau (1873) concluded experimentally that interfaces of soap bubbles always satisfy three geometric conditions [9, 11–13]:

1. Only 3 interfaces can meet at a point, creating Plateau borders; the amount by which a border is curved inward or outward is determined by the difference in pressure on either side (Young-Laplace equation).
2. The tangential angles between the Plateau borders is 120° ($2\pi/3$).
3. Four Plateau borders, each formed by the intersection of three surfaces, are joined at vertices creating an angle equal to $109^\circ 28'16''$ (arccos[-1/3]), called the Maraldi angle.

These elegant rules can be used to explain the interactions among clustered soap bubbles. From a geometric perspective, these interactions can be described quantitatively using three equations (A, B, and C represent centers of the bubbles and r_A, r_B, and r_C are their respective radii) [9]:

$$\frac{1}{r_B} = \frac{1}{r_A} + \frac{1}{r_C} \tag{1}$$

$$|AB|^2 = r_A{}^2 + r_B{}^2 - 2r_A r_B \cos\left(\frac{\pi}{3}\right) \tag{2}$$

$$|AC|^2 = r_A{}^2 + r_C{}^2 - 2r_A r_C \cos\left(\frac{2\pi}{3}\right) \tag{3}$$

Equation (1) may be derived from the Young-Laplace equation, eqn. (4), in which p represents excess pressure and σ represents surface tension (which is constant for all soap bubbles) at an interface , r_1 and r_2 are the principle radii of curvature, which, in a soap bubble, are equal, so eqn. (4) can be replaced by eqn. (5) [9, 14].

$$p = \sigma\left(\frac{1}{r_1} + \frac{1}{r_2}\right) \tag{4}$$

$$p = \frac{2\sigma}{r} \tag{5}$$

Pressure is proportional inversely to the radius of curvature eqn. (5). This means that large bubbles contain low excess pressure, while small bubbles contain high excess pressure [10]. Coalescing bubbles are surrounded by three different pressures; inside bubble *A* (pA), inside bubble *B* (pB), and everywhere else (pC) [9].The excess pressure between pA and pC, pAC, must be equal to the excess pressures between the two other regions, pBC and pAB [9, 10]:

$$pAC = pBC + pAB \tag{6}$$

Therefore,

$$\frac{2\sigma}{r_A} = \frac{2\sigma}{r_B} + \frac{2\sigma}{r_C} \tag{7}$$

and

$$\frac{1}{r_A} = \frac{1}{r_B} + \frac{1}{r_C} \tag{8}$$
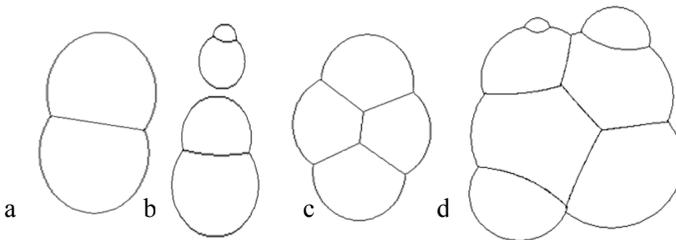
Figure 2:   Computer generated output depicting Plateau borders created between: a) two identical bubbles, b) two different-sized bubbles, c) 4 identical bubbles, known as Lozenge configuration, and d) clustered different-sized bubbles. The output was generated using an algorithm that incorporated eqns. (1), (2), and (3).

Two cases are considered, one with equal-sized bubbles and one with different-sized bubbles. When equal-sized bubbles meet, no differential is produced, so the Plateau border will be flat, fig. 2a and 2c [9, 10, 15]. The radius

of curvature (r_C) will be infinite. When unequal-sized bubbles meet, the smaller bubble, which has higher pressure, will push into the larger bubble, fig. 2b and 2d [9, 10, 15]. The boundary between the bubbles created by the radius of curvature (r_C) will be curved, with the concave side toward the larger bubble [9, 10, 15].

3 Descartes and close-packing

Mathematicians strive to find "optimal" solutions; whether an area, distance, or shape, minima and maxima are sought. Close-packing is an arrangement wherein the ratio area covered: total area is optimized [13, 16]. Most studies concentrate on packing circles within a fixed area [16]. Solving packing problems such as circles within circles was made possible by Descartes, who showed that curvature is proportional inversely to radius and described 'Descartes configurations' [17]. In these configurations no three circles share a common tangent [16, 17]. Circle-packing has captured the interest of myriad mathematicians and scientists who sought to solve what was referred to as the "Descartes circle theorem" or "Kissing circle theorem" [17, 18].

Circle packing may be described as an arrangement in which circles assume a specific tangency pattern [16]. The simplest close-circle-packing patterns are square and triangular tessellations, fig. 3 [13, 16].
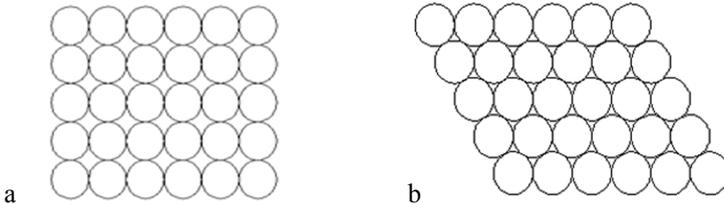
Figure 3:   Circle packing tessellation patterns a) square, wherein four circles meet around one point and b) triangular, wherein only three circles meet around one point.

The densest Euclidean (2-D plane) packing configuration is achieved with triangular tessellation patterns [13, 16]. Only three circles meet around one point [16]. These resemble the close-packing patterns that are observed in nature on a macroscopic and microscopic scale, such as the honeycombs cells and single-crystal lattice respectively [19, 20].

4 Sea urchins and analogy

4.1 Why sea urchins?

Sea urchins have evolved processes and patterns that resemble the close-packing and arrangements exhibited by interacting soap bubbles. Sea urchin skeletons may be considered as 3-dimensional jigsaw puzzles.
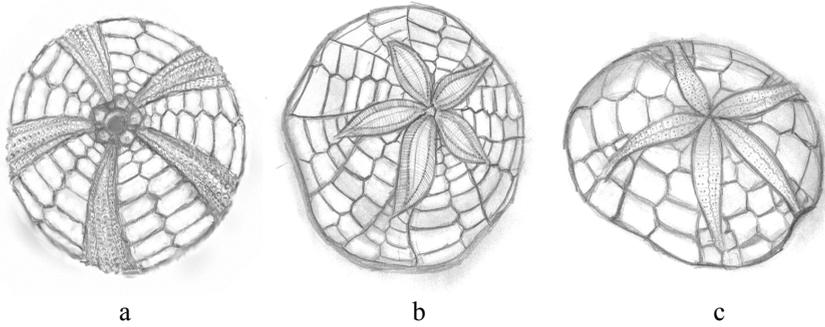
Figure 4:   Illustrations of a) sea urchin, b) sand dollar, and c) heart urchin skeletons.

They present two surfaces: aboral (top) and oral (bottom) [21]. The aboral surface houses the apical system, where new plates are added [21]. New plates stimulate the growth and a relative downward shift of older plates [22]. The apical system, itself, comprises 10 plates arranged in an alternating ring, five ocular and five genital, which surround a central plate [8]. New plates are inserted juxtaposed to the ocular plates, resulting in five alternating biserial columns of ambulacral plates (porous) and interambulacral plates [23]. This arrangement produces the pentamerous symmetry exhibited by all living echinoids (sea urchins, sand dollars, and heart urchins), fig. 4 [8].

4.2 Soap bubble analogy

The current study stems from the conceptual model proposed by Thompson and computer program developed by Raup in 1968. Raup proposed that plates
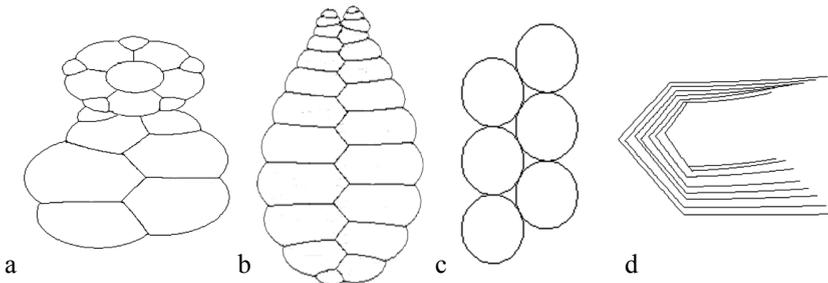
Figure 5:   The four processes essential in modelling sea urchin skeleton growth. a) plate addition – plates are added at the top, the apical system; b) plate shift – new plate addition imparts a shift to older plates, down the columns; c) plate gapping – before plates grow, they separate, separation being modelled using close-packing interactions; d) plate growth – plates grow peripherally, their boundaries being modelled using soap bubble interactions.

behave in a manner similar to soap bubbles interacting in a close-packing configuration and demonstrated that soap bubble interactions can be used as a model for producing these plate patterns [2]. His model explored the effect on plate configurations imparted by plate supply (new plate addition) and peripheral accretion [2]. But he did not attempt to use the soap bubble analogy for plate interactions [2]. Instead, Raup depicted plate margins using straight lines and assumed that angles between boundaries were coequal [2]. He made no attempt to simulate the curved boundaries present where different-sized plates interact. Although lacking in several details, his computational study constituted a monumental step in using computers to explain natural processes.

In this study, we introduce a computational model that incorporates fundamental mathematical and physical principles associated with soap bubble interactions combined with biological constraints associated with sea urchin skeleton growth. We consider 4 processes: plate addition, plate shifting, plate gapping, and plate growth, fig. 5.

4.3 Proviso

4.3.1 Plate addition
New plates are inserted at the apical system; in our computational model the apical system is created by interacting soap bubbles in a ring, with the genital plates in the inner ring and larger than the ocular plates in the outer ring. This interaction shows remarkable similarities to the apical system in *Arbacia punctulata*, fig. 6. The apical structure presents the first step in the skeleton formation. It determines the locations for the new plates; they are added contiguous with the ocular plates; in our computational model, plates are added at the intersection point between the ocular and genital plates fig. 5a.

a   b   c
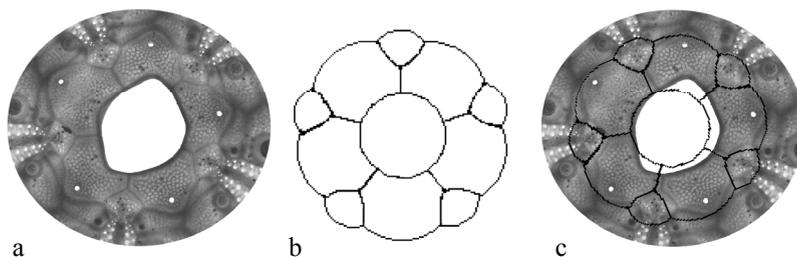
Figure 6:   a) a photograph of an apical system of *Arbacia punctulata*, b) apical system created using the computational model, and c) b is superimposed onto a.

4.3.2 Plate shift
Our computational model works in two dimensions; thus, the movement occurs away from the apical system. This is observed as a relative downward shift of the plates in the columns, fig 5b. New plates added at the top of the column push onto adjacent plates, thus forcing the older plates to shift. This is an essential
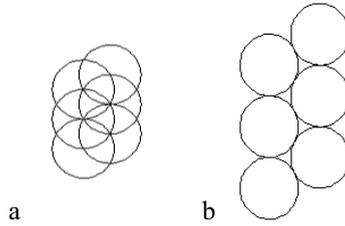
Figure 7:   a) Computer simulation depicting the overlapping positions for interacting plates, here drawn as circles; b) close-packing configuration, simulating the gapping required for plates.

step, because plate location provides the curvature and shape information for the whole skeleton.

4.3.3 Plate gapping

Plate gapping occurs before plate growth [24]. In our computational model, gapping occurs using the circle packing analogy. The plates that are in the overlapping positions initially will separate from neighbouring interactions to a close-packing configuration, fig. 7. This 'frees' plates from neighbouring interactions, allowing them to grow and shift before they re-interact.

4.3.4 Plate growth

Plate growth occurs through peripheral accretion onto each existing plate [22, 25, 26]. Depending on their position in the skeleton, plates exhibit different growth patterns and rates [25, 27]. Growth lines on a plate correspond with, and so, can be used to enumerate plates inserted subsequent to it [26]. Thus, in our computational model plate growth is initiated after new plates are added and
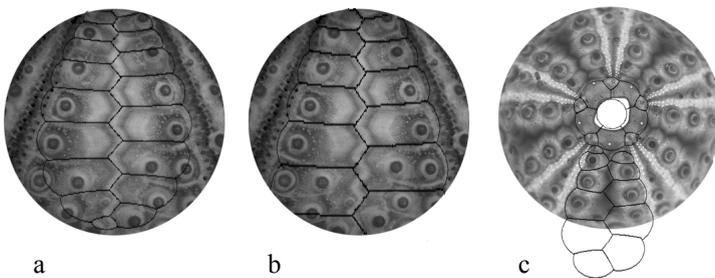
Figure 8:   Results from our computational model show similarities between the interambulacral plate patterns of *A. punctulata* and the soap-bubble analogy: a) a slow plate growth matches the adoral plates; b) faster growth rates match more closely the aboral plates. c) a 2D simulation of a young *A. punctulata* is superimposed onto the whole skeleton, emphasizing the similarities between our computational model and plate patterns.

gapping has occurred. Once plate growth occurs, which is simulated by increasing radii, each plate interacts according to the soap bubble analogy, forming a new boundary, fig. 5d. Growth is modelled using a parabolic growth function [2]. By changing the growth function, the computational model can provide insight into the growth rate of specific sea urchin species, fig. 8.

5 Prospectus

The soap bubble analogy provides a model that can be used to explain the patterns that are observed in sea urchin skeletons fig. 7. We intend to use our computational model to describe the evolutionary morphological changes observed in sea urchin skeletons. Sea urchins and their sister taxa, sand dollars, start with virtually identical morphologies at the juvenile stage and then diverge into domed and flat disc shapes, respectively. We believe that our computational model, through the 4 plate processes (addition, shift, gapping and growth) can be used to explain these morphological changes.

6 Methodology

The computer program was developed using the technical computing environment *Mathematica 4.0*. Illustrations and digital images were created and captured by M. Abou Chakra.

Acknowledgements

References

[1]   Thompson, D.A.W., *On Growth and Form*, An abridged ed. Press Syndicate of the University of Cambridge: Cambridge, Unite Kingdom, pp. 945, 1961.
[2]   Raup, D.M., Theoretical morphology of echinoid growth. *Journal of Paleontology*, 42, pp. 50–63, 1968.
[3]   Moss, M.L. and Meehan, M., Growth of the echinoid test. *Acta Anatomica*, 69, pp. 409–444, 1968.
[4]   Seilacher, A., Constructional morphology of sand dollars. *Paleobiology*, 5(3), pp. 191–221, 1979.
[5]   Telford, M., Domes, arches and urchins: the skeletal architecture of echinoids (Echinodermata). *Zoomorphology*, 105, pp. 114–124, 1985.
[6]   Barron, C.J., *The Structural Mechanics and Morphogenesis of Extant Regular Echinoids Having Rigid Tests*. Zoology. Vol. Doctor of Philosophy. University of California at Berkeley, pp. 285, 1991.

[7]   Ellers, O., A mechanical model of growth in regular sea urchins: predictions of shape and a developmental morphospace. *Proceedings: Biological Sciences*, 254(1340), pp. 123–129, 1993.

[8]   Hyman, L.H., *The Invertebrates: Echinodermata*. The coelomate bilateria. Vol. IV. McGraw-Hill Book Company: New York, pp. 763, 1955.

[9]   Isenberg, C., *The Science of Soap Films and Soap Bubbles*. Tieto Ltd.: England, pp. 188, 1978.

[10] Boys, S.C.V., *Soap Bubbles and The Forces Which Mould Them*. Doubleday Anchor Books: Garden City, N.Y., pp. 156, 1959.

[11] Morgan, F., Soap bubbles in r^2 and in surfaces. *Pacific Journal of Mathematics*, 165(2), pp. 347–361, 1994.

[12] Fischer, F., Four-bubble clusters and Menelaus' theorem. *American Journal of Physics*, 70(10), pp. 986–991, 2002.

[13] Aste, T. and Weaire, D.L., *The Pursuit of Perfect Packing*. Institute of Physics Pub: Bristol Philadelphia, Pa, pp. 136, 2000.

[14] Young, T., An essay on the cohesion of fluids. *Philisophical Transactions of the Royal Society of London*, 95, pp. 65–87, 1805.

[15] Durikovic, R., Animation of soap bubble dynamics, cluster formation and collision. *eurographics 2001*, 20(3), 2001.

[16] Stephenson, K., *Introduction To Circle Packing : The Theory of Discrete Analytic Functions*. Cambridge University Press: Cambridge, UK ; New York, pp. 356, 2005.

[17] Langarias, J.C., Mallows, C.L., and Wilks, A.R., Beyond the Descartes circle theorem. *The American Mathematical Monthly*, 109(4), pp. 338–361, 2002.

[18] Coxeter, H.S.M., *Introduction To Geometry*, 2nd ed. Wiley: New York, pp. 469, 1969.

[19] Tóth, F., What the bees know and what they do not know. *Bulletin of the American Mathematical Society*, 70, pp. 468–481, 1964.

[20] Lovett, D.R. and Tilley, J., *Demonstrating Science with Soap Films*. Institute of Physics Publishing: Bristol, Philadelphia, pp. 204, 1994.

[21] Smith, A.B., *Echinoid Palaeobiology*. Special topics in palaeontology. Allen & Unwin: London, pp. 190, 1984.

[22] Gordon, I., The development of the calcareous test of *Echinus miliaris*. *Philisophical Transactions of the Royal Society of London. Series B, Containing Papers of Biological Character*, 214(1926), pp. 259–312, 1926.

[23] Jackson, R.T., *Phylogeny of the Echini, with a Revision of Palaeozoic Species*. Memoirs of the Boston Society of Natural History. Vol. 7. The Society: Boston, pp. 491, 1912.

[24] Dafni, J., A biomechanical model for the morphogenesis of regular echinoid tests. *Paleobiology*, 12(2), pp. 143–160, 1986.

[25] Deutler, F., Uber das Wachstum des seeigetckeletts. *Zoologische Jahrbcher*, 48, pp. 119–200, 1926.

[26] Pearse, J.S. and Pearse, V.B., Growth zones in the echinoid skeleton. *American Zoologist*, 15, pp. 731–753, 1975.

[27] Märkel, K., Experimental morphology of coronar growth in regular echinoids. *Zoomorphology*, 97(1-2), pp. 31–52, 1981.